

Enhancement of photovoltaic effect in $\text{La}_{0.9}\text{Sr}_{0.1}\text{MnO}_3/\text{Si}$ heterojunction by side illumination

Jie Xing¹, Kun Zhao^{2,3,4}, Guo Zhen Liu¹, Meng He¹,
Kui Juan Jin¹ and Hui Bin Lu^{1,4}

¹ Beijing National Laboratory for Condensed Matter Physics, Institute of Physics, Chinese Academy of Sciences, Beijing 100080, People's Republic of China

² Department of Mathematics and Physics, China University of Petroleum, Beijing 102249, People's Republic of China

³ International Center for Materials Physics, Chinese Academy of Sciences, Shenyang 110016, People's Republic of China

E-mail: hblu@aphy.iphy.ac.cn (Hui Bin Lu) and zhk@cup.edu.cn (Kun Zhao)

Received 27 July 2007, in final form 14 August 2007

Published 21 September 2007

Online at stacks.iop.org/JPhysD/40/5892

Abstract

The side-illumination-enhanced photovoltaic effect has been studied in $\text{La}_{0.9}\text{Sr}_{0.1}\text{MnO}_3/\text{Si}$ heterojunctions fabricated by laser molecular beam epitaxy. When a He–Ne laser illuminated the $\text{La}_{0.9}\text{Sr}_{0.1}\text{MnO}_3$ film surface, a stable photovoltage was produced and the responsivity is $\sim 0.17 \text{ mV mW}^{-1}$. An enhancement of the photovoltaic effect occurred when the $\text{La}_{0.9}\text{Sr}_{0.1}\text{MnO}_3/\text{Si}$ interface was illuminated directly by side illumination, and the steady responsivity reached $\sim 6.87 \text{ mV mW}^{-1}$. This work demonstrates an effective way to improve the photovoltaic responsivity of the perovskite oxide heterojunctions.

1. Introduction

Photocarriers injection induced the resistance or magnetic or electrical changes to open up a new way of exploring the mechanism in the strong correlated electronic systems [1–8]. Perovskite-based p–n junctions are sensitive to light illumination, revealing their potential for photonic device applications [9–17]. Conventional semiconductor p–n theory, in which majority carriers and the built-in field dominate the formation of photovoltage, was applied to explain the photovoltaic effect in perovskite-based p–n junctions: at zero bias, photogenerated electron–hole pairs are driven by the built-in field in the depletion region, forming the photovoltage or photocurrent when the device is open or short circuited, respectively [12–17]. Furthermore, the spatial distributions of the electrostatic potential across perovskite-based p–n junction interfaces indicated the presence of a depletion layer and a built-in electric field within the junctions [18, 19].

Previously we had developed the ultrafast photovoltaic detector based on epitaxial perovskite oxide thin films on Si substrates and found nanosecond and picosecond

response time in $\text{La}_{0.7}\text{Sr}_{0.3}\text{MnO}_3/\text{Si}$ [14], $\text{SrTiO}_{3-\delta}/\text{Si}$ [15] and $\text{BaNb}_{0.3}\text{Ti}_{0.7}\text{MnO}_3/\text{Si}$ p–n heterojunctions [16], respectively. In this paper, we aim to improve the responsivity of perovskite-based p–n junctions. For this purpose, the film/substrate interface is illuminated directly (side illumination), which is different from the previous work where the junction was illuminated at the air/film interface (front illumination) [9–17].

2. Experimental procedure

The perovskite-based heterojunction was fabricated by growing a 200 nm thick $\text{La}_{0.9}\text{Sr}_{0.1}\text{MnO}_3$ (LSMO) film on a n-type Si substrate with a resistivity of $4 \Omega \text{ cm}$ and a carrier concentration of $1 \times 10^{16} \text{ cm}^{-3}$ using a computer-controlled laser molecular beam epitaxy system equipped with an *in situ* reflection high-energy electron diffraction (RHEED) system. To improve the interface quality, a two-step method was applied to prevent the formation of a SiO_2 interface layer as described in our previous work [14]. Firstly, about a two-unit-cell thick LSMO film was deposited on the substrate surface at room temperature. The Si substrate was then raised to 620°C at the base pressure of $\sim 1 \times 10^{-5} \text{ Pa}$ before the deposition

⁴ Author to whom any correspondence should be addressed.

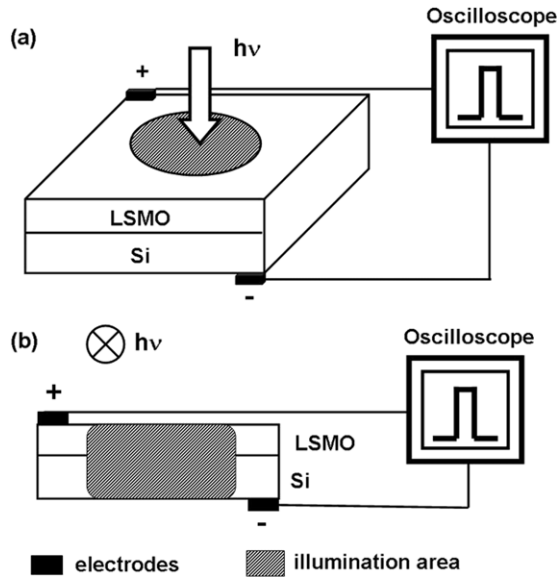


Figure 1. Schematic circuits of (a) front and (b) side illumination for the photovoltaic measurement.

of the LSMO film started again. An *in situ* RHEED system and a CCD camera were used to monitor the growth process of the LSMO thin films. After the RHEED streak pattern of the initial two-unit-cell thick LSMO film appeared, the LSMO was continuously deposited under a pressure of 3×10^{-2} Pa, which was created by an active oxygen source ($\sim 10\%$ O).

The whole sample was $5 \times 6 \text{ mm}^2$ in area and $\sim 0.4 \text{ mm}$ in thickness. For the photovoltaic measurement, two indium electrodes of 1 mm^2 were applied on the corner of the LSMO film and the Si substrate. As shown in figure 1, a He–Ne laser of wavelength $\lambda = 632.8 \text{ nm}$ and power density of 1 mW mm^{-2} was used to illuminate the LSMO film surface (front illumination) and the LSMO/Si interface (side illumination). The diameter of the light spot was 3 mm . During the measurement all the electrodes were kept in the dark to avoid the photovoltaic effect due to contact barrier. The effective area was about 28.3 mm^2 and 1.2 mm^2 for the front and side illumination, respectively. Thus, the on-sample power was 28.3 mW for the front condition and 1.2 mW for the side one. The open-circuit photovoltage was recorded by a 500 MHz sampling oscilloscope (Tektronix TDS3052B) with an input impedance of $1 \text{ M}\Omega$.

3. Results and discussion

The Hall effect study revealed that LSMO was actually hole-doped and the carrier concentration was $1.19 \times 10^{18} \text{ cm}^{-3}$. Therefore, LSMO and n-type Si constructed a p–n junction. This was confirmed by the asymmetric current–voltage relations against the polarity of the bias voltage in figure 2, which was a typical feature of p–n junctions and generally ascribed to the presence of interfacial potential due to carrier diffusion.

Figure 3 exemplifies the photovoltaic responsivity R of the LSMO/Si junction as a function of time under the illumination of a continuous He–Ne laser. R is calculated by the recorded photovoltage divided by the on-sample power. Since the

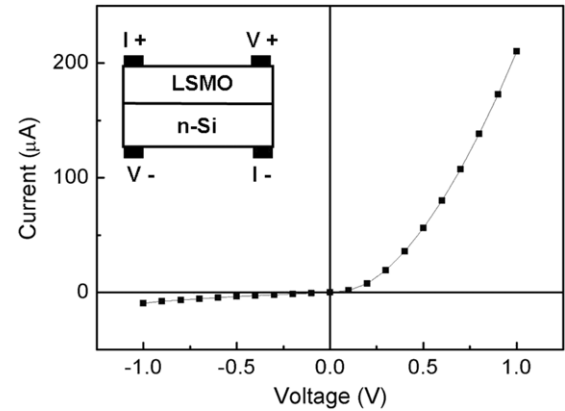


Figure 2. Current–voltage characteristics of the LSMO/Si junction measured at room temperature. The inset shows a schematic illustration of the sample measurement.

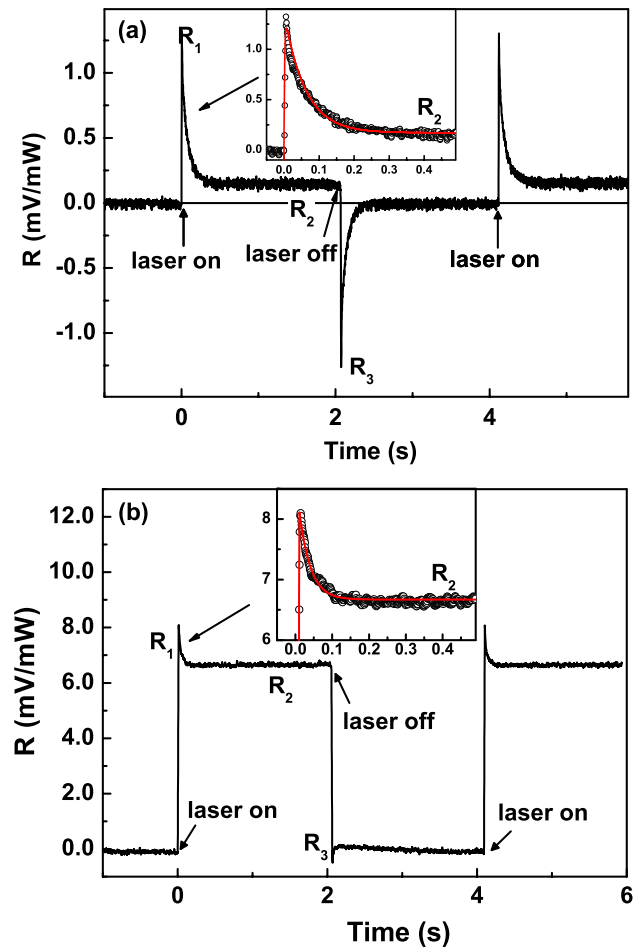


Figure 3. Responsivity of LSMO/Si under (a) front and (b) side illumination of a He–Ne laser.

(This figure is in colour only in the electronic version)

632.8 nm photon energy is larger than the band gaps of LSMO and Si, electrons in the valence bands of the LSMO and Si absorbed the He–Ne laser photons and made a transition into the conduction bands. Thus holes in the valence bands and electrons in the conduction bands were created, respectively. Those excess carriers created in the space charge region or within one diffusion length near the space charge region

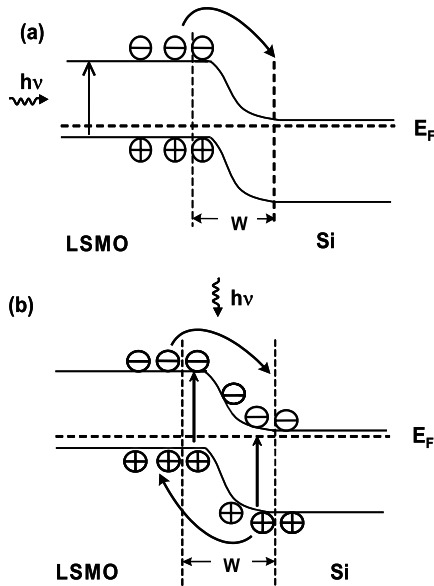


Figure 4. Schematic diagram of the movement of carriers under (a) front and (b) side illumination.

can be separated by the built-in field, resulting in holes being swept into the LSMO film and electrons into the Si substrate. Eventually, a photovoltage between the two electrodes occurs.

As shown in figures 3(a) and (b), the responsivity is dependent on the illumination time. After the laser is switched on, the response increases suddenly to a transient maximum R_1 following a steady value R_2 . On turning off the laser there was an immediate transient signal R_3 in the opposite direction, which then decayed slowly to zero. These changes occur quite reversibly and reproducibly, and no degradation was seen after switching on many times. A careful analysis indicates that the R - t curve can be well described by a rise part ($R \propto 1 - \exp(-t/\tau_1)$) and a fall part ($R \propto \exp(-t/\tau_2)$). The former corresponds to the rapid increase in R while the latter to the slow decay to steady R_2 . The response times τ_1 and τ_2 are ~ 2 ms and ~ 60 ms for front illumination and ~ 1 ms and ~ 30 ms for side illumination, respectively.

This behaviour is different from that reported by Sun, where no transient peak was observed [12]. Although the pyroelectric effect has been suggested to explain the transient phenomenon corresponding to light-on and light-off in other materials, e.g. BaTiO₃ crystals and BaTiO₃/Si heterostructures [20, 21], the underlying mechanism remains an open question for manganite-based heterojunctions. In this paper, special attention is paid only to the steady-state photovoltaic responses under different illumination modes.

The width of the depletion region calculated in the abrupt p-n junction model is about hundreds of nanometres at zero bias and most of the depletion region is located at the Si side as illustrated in figure 4 [14–17]. For front illumination (figure 3(a)), the LSMO film absorbed a great part of the photons and only a little part of photons can reach the Si side. Thus, the photovoltage signal mostly came from the electrons at the LSMO side drifting to the Si substrate (figure 4(a)). In addition, based on the formula $L = (\kappa T \mu \tau / q)^{1/2}$ [22], the diffusion length L of photocarriers is estimated to be ~ 50 nm for electrons in LSMO by inserting the carrier mobility μ

of $1 \text{ cm}^2 \text{ V}^{-1} \text{ s}^{-1}$ obtained by the Hall effect measurement, the carrier lifetime τ of ~ 1 ns [14], the temperature T of 300 K, Boltzmann's constant κ and the electron charge q . Compared with the LSMO film thickness the limited diffusion length suggested that many of the electrons recombined before they reached the depletion region. So a lower steady R_2 of $\sim 0.17 \text{ mV mW}^{-1}$ occurs when the LSMO surface is illuminated.

In contrast, for the side illumination condition the He-Ne laser directly impinged onto the LSMO/Si interface and generated electron-hole pairs at both LSMO and Si sides as illustrated in figure 4(b). Driven by the built-in field, electrons in LSMO drifted to the Si side and holes in Si to the LSMO side. Two kinds of carriers jointly contributed to the photo response. Following the above formula, we obtained $L \approx 0.5$ mm for holes in Si, inserting $\mu \approx 500 \text{ cm}^2 \text{ V}^{-1} \text{ s}^{-1}$ and $\tau \approx 130 \mu\text{s}$ [22], which indicated that most of the holes in Si can reach the depletion region. Eventually the collection of photo generated carriers was improved leading to a much higher steady value of $R_2 \approx 6.87 \text{ mV mW}^{-1}$ (figure 3(b)).

4. Summary

In summary, side-illumination-induced enhancement of the photovoltaic response of the LSMO/Si heterojunction was investigated. The photovoltaic responsivity can reach 6.87 mV mW^{-1} under side illumination, which is much larger than 0.17 mV mW^{-1} under front illumination. The mechanism of such an effect is proposed. This work manifests a simple way of improving the photo responsivity.

Acknowledgments

This work has been supported by the National Natural Science Foundation of China (Grant Nos 50672132 and 60576015), the National Basic Research Programme of China and the Key Project of Chinese Ministry of Education (No 107020).

References

- [1] Kiryukhin V, Casa D, Hill J P, Keimer B, Vigliante A, Tomioka Y and Tokura Y 1997 *Nature* **386** 813
- [2] Zhao Y G, Li J J, Shreekala R, Drew H D, Chen C L, Cao W L and Lee C H 1998 *Phys. Rev. Lett.* **81** 1310
- [3] Matsuda K, Machida A, Moritomo Y and Nakamura A 1998 *Phys. Rev. B* **58** R4203
- [4] Averitt R D, Lobad A I, Kwon C, Trugman S A, Thorsmille V K and Taylor A J 2001 *Phys. Rev. Lett.* **87** 017401
- [5] Ogasawara T, Kimura T, Ishikawa T, Kuwata-Gonokami M and Tokura Y 2001 *Phys. Rev. B* **63** 113105
- [6] Dai J M, Song W H, Du J J, Wang J N and Sun Y P 2003 *Phys. Rev. B* **67** 144405
- [7] Zhao K, Jin K J, Huang Y H, Zhao S Q, Lu H B, He M, Chen Z H, Zhou Y L and Yang G Z 2006 *Appl. Phys. Lett.* **89** 173507
- [8] Katsu H, Tanaka H and Kawai T 2000 *Appl. Phys. Lett.* **76** 3245
- [9] Watanabe Y and Okano M 2001 *Appl. Phys. Lett.* **78** 1906
- [10] Muraoka Y, Muramatsu T, Yamaura J and Hiroi Z 2004 *Appl. Phys. Lett.* **85** 2950
- [11] Muramatsu T, Muraoka Y and Hiroi Z 2004 *Solid State Commun.* **132** 351

- [12] Sun J R, Shen B G, Sheng Z G and Sun Y P 2004 *Appl. Phys. Lett.* **85** 3375
- [13] Sun J R, Lai C H and Wong H K 2004 *Appl. Phys. Lett.* **85** 37
- [14] Lu H B, Jin K J, Huang Y H, He M, Zhao K, Cheng B L, Chen Z H, Zhou Y L, Dai S Y and Yang G Z 2005 *Appl. Phys. Lett.* **86** 241915
- [15] Zhao K, Huang Y H, Zhou Q L, Jin K J, Lu H B, He M, Cheng B L, Zhou Y L, Chen Z H and Yang G Z 2005 *Appl. Phys. Lett.* **86** 221917
- [16] Huang Y H, Zhao K, Lu H B, Jin K J, Chen Z H, Zhou Y L and Yang G Z 2006 *Appl. Phys. Lett.* **88** 061919
- [17] Zhao K, Jin K J, Lu H B, Huang Y H, Zhou Q L, He M, Chen Z H, Zhou Y L and Yang G Z 2006 *Appl. Phys. Lett.* **88** 141914
- [18] Tian H F, Sun J R, Lu H B, Jin K J, Yang H X, Yu H C and Li J Q 2005 *Appl. Phys. Lett.* **87** 164102
- [19] Tian H F, Yang H X, Zhang H R, Li Y, Lu H B and Li J Q 2006 *Phys. Rev. B* **73** 075325
- [20] Chynoweth A G 1956 *Phys. Rev.* **102** 705
- [21] Dharmadhikari V S and Grannemann 1982 *J. Appl. Phys.* **53** 8988
- [22] Sze S M 1999 *Physics of Semiconductor Device* (New York: Wiley)